A blast wave generator in MARTEL facility to simulate overpressure induced by solid rocket motor at lift-off

C. Bresson, H. Foulon **, H. Lambaré ***, M. Pollet****, P. Malbéqui**

**Onera, 29 avenue de la Division Leclerc, 92322 Châtillon Cedex, France*
***Aeroacous consult, 17bis, rue Madeleine Vernet, 37270 MONTLOUIS sur Loire, France*
****Cnes, Rond Point de l'Espace Courcouronnes, 91023 Evry Cedex, France*
*****ASTRIUM Space Transportation, BP3002 - 78133 Les Mureaux Cedex, France*

Abstract

The ignition of the solid rocket motor of heavy launch vehicles induces a strongly impulsive wave at lift-off, which may generate constraints on the payload and the equipments. To implement research studies in the field of blast wave, it was decided to develop in the MARTEL facility a system able to simulate this blast wave. The objective is to characterize the phenomenon, to validate numerical methods and to assess reduction systems. This paper describes the blast wave generator principle and its capabilities obtained in free field and in presence of a trench.

1. Introduction

At lift-off, the jet noise generated by the motors of heavy launch vehicles produces a severe environment where the loads induced may damage payload and equipments. Powerful launch vehicles, such as Ariane 5, involve an increase of the external sound pressure level, where the specifications of the satellites covered by the fairing have to be accurately fulfilled. The MARTEL facility, funded by CNES and installed in CEAT of Poitiers University, has been developed in 1996 as part of the Research and Technology CNES program. The research group AEID (Acoustique et Environnement Induits au Décollage) was created in 1990 to understand the noise radiation mechanisms associated with hot supersonic jets and to design noise reduction systems. It is composed by ASTRIUM, CEAT/MARTEL from University of Poitiers, CNES, ECL, ONERA and PPRIME. In this frame, number of experiments carried out in MARTEL facility allowed us to develop semi-empirical methods and to validate numerical simulations. The MARTEL facility produces subsonic or supersonic jets, cold or hot, and is used to carry out both fundamental and applied research studies. The facility is characterized by a testing hall surrounded by a huge anti-noise embankment, with an efficient acoustic treatment to ensure a semi-anechoic ambience (Fig. 1). Efficient systems to reduce the jet noise have been designed and assessed, including the water injection in the launch pad together with the trench extension [1].

On the other hand, the ignition of the Solid Rocket Motor (SRM) of heavy launch vehicles still induces a strongly impulsive wave at lift-off. In practice, this overpressure wave excites the low frequency mechanical modes of the launcher, leading to dynamic and quasi-static loads to the payloads, which have to be qualified to these loads. The induced loads depends on the level and frequency of the overpressure wave, and on the launcher configurations and the payload. The mechanism appears during the launch vehicle take-off where the pressure in the engine combustion chamber undergoes a rather fast increase until the steady-state chamber pressure is achieved. The magnitude of the over-pressure depends on the chamber pressure derivative [2]. The blast wave generated on the launch pad is characterized by two components: the Ignition Over-Pressure (IOP) impinging on the bottom of the trench and radiating from the opening of the trench entrance from apertures at the entry of the duct and the Duct Over-pressure (DOP) propagating from the downstream exit of the duct (*i;e.*, the trench exhaust) as illustrated in figure 2. Complementary tools are available to analyse the blast–wave. Analytical methodology provides some physical understanding of the blast wave mechanism, while thanks to progress in numerical methods and computer resources, computations become powerful tools to analyse launch vehicle environment [3, 4]. Numerical simulations performed at full scale of the launcher gives satisfactory results compared to the measurements, in views of the high complexity of the flow fields and the launch pad geometry [5]. Measurements on rocket engine at reduced scale provide realistic conditions to simulate a representative blast wave. Experiments performed in Centre Fauga Mauzac of Onera with a propellant engine exhibit the blast-wave propagation in free jet and in presence of the flame trench, and the

recombustion phenomenon of propellant combustion products with ambient air, which may increase the magnitude of the overpressure [6, 7]. Numerical simulations based on CFD with reactive LES computations including confined water in the trench are in a good agreement with these experiments, showing the cool down of the plume temperature which quenches the recombustion [8]. However, such experiments and CFD simulations remain expensive and CPU time consuming in the framework of research activities to allow numerous configurations for designing reduction systems. So, to implement research studies in this field, Cnes decided to develop a system able to simulate the blast wave phenomenon in the MARTEL facility. The objective is to characterize the phenomenon, to validate numerical methods and to assess reduction systems. The generator has been studied in cooperation with Astrium, CEAT, CNES, LCD (Laboratoire de Combustion et Détonique of CNRS, PPRIME Institute, Poitiers, France) and Onera.
This paper describes the blast wave generator principle in Section 2. Its capabilities for cold and hot gas in the MARTEL facility are presented in Section 3. Section 4 details the measurements and the results obtained in presence of a trench.

Figure 1: Martel Facility in CEAT

Figure 2: DOP ring generated at the duct exit (courtesy of CNES).

2. The blast wave generator

2.1. Principle

Figure 3a shows the generator set up in the Martel facility. Figure 4 details the diagram of the blast wave generator. The system is composed of one tank and a chamber with a variable volume from 2 to 9.5 litres. The tank has a spherical volume of 100 litres which provides the energy supply and a cylindrical volume which represents the launch body. A diaphragm, which separates the chamber from the cylindrical volume, is struck by remote control at a prescribed pressure. Changing the chamber volume from 2 to 9.5 litres allows us to adjust the pressure rise. This parameter plays a significant role in the generator, the magnitude of the overpressure depending on the rate of change of the chamber pressure. The chamber ends with a convergent-divergent nozzle, cone-shaped with a 60 mm exit diameter, opening outside. An adjustable support with a set of block elements allows keeping the same distance of 1,53m between the nozzle exit and the ground, whatever the length of the variable chamber is. Five pressure sensors are located inside the generator: in the sphere, P_{Sphere}, on the top and bottom of the cylinder, $P_{Cyl.-Top}$ and $P_{Cyl.-Bottom}$, in the interior of the chamber close to the divergent and at its exit, $P_{Chamber-Div.}$ and $P_{Chamber-Exit}$.
Two ways of working are possible with the generator: cold gas and hot gas. In the first configuration the tank is filled with air under pressure up to 200 bars at the temperature of about 290 K. In the second configuration, the hot jet is produced by the deflagration of methane-air mixture ignited inside the spherical volume, under pressure up to 100 bars and at a temperature of about 2500 K. The cold gas configuration provides representative shape of the overpressure and its implementation is easier, while the hot jet gives a more realistic description in pressure and temperature of the mixed gas relative to the combustion of a SRM propellant. This point is essential in the study of reduction systems, including water injection or spray injection, which are very sensitive to the temperature of the gas, involving both kinematical and thermal energy transfers. While the cold jet configuration is the first step to demonstrate the capabilities and the acceptance of generator, the main effort focuses on the hot gas configuration. The principle of the generator is to turn up the pressure upstream of the nozzle exit and to set off the disk rupture (diaphragm) at the prescribed pressure. In cold jet configuration, the pressure is obtained with a compress air device while in the hot jet one, the prescribed pressure results from the air-methane combustion after ignition of a spark plug. A code provided by LCD based on isochoric combustion described the thermodynamic characteristics of the combustion components after ignition (CO2, H2O, N2, O2, CO, H2, OH, H, O), as function of the initial pressure

and the richness of the air–methane mixture. In practice, the generator works with a stœchiometric air-methane mixture of richness of 1 and an initial pressure of 10 bars, including 1 mole of methane and 9.52 moles of air, leading to the following chemical equation:

$$CH4+202+7{,}52N2 \rightarrow C02 + 2H20+7{,}52N2$$

a) Generator in “free jet” configuration b) Generator in presence of the trench

Figure 3: Blast-wave generator set up in the Martel facility.

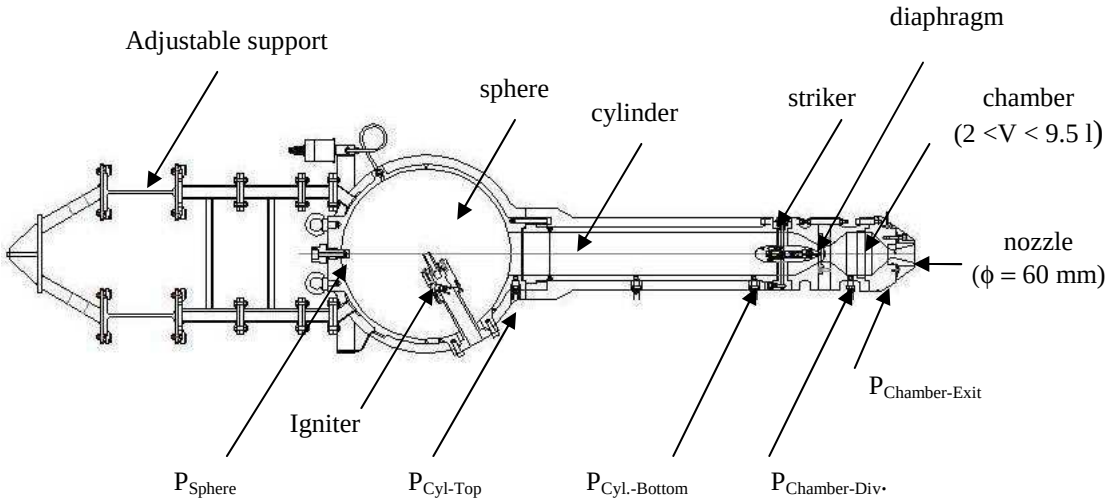

Figure 4: Diagram of the blast wave generator including pressure sensors.

2.2 Performances of the blast wave generator

Preliminary tests have been carried out to adjust the nominal pressure and volume of the chamber of the generator to obtain a representative pressure rise compared to the full scale configuration. The pressure gradient is obtained by finite difference: $\frac{dP}{dt} = \frac{P_{90} - P_{10}}{t_{90} - t_{10}}$, where t_{10} and t_{90} correspond to the times where the pressure reach P_{10} and P_{90}, 10% and 90% of the maximum pressure, respectively.

Cold gas configuration

Figure 5 plots the pressure rise measured in the cylindrical part of the tank on $P_{Chamber\text{-}Div}$. As expected, it is observed that the pressure rise increases when increasing the pressure and when reducing the volume of the chamber.

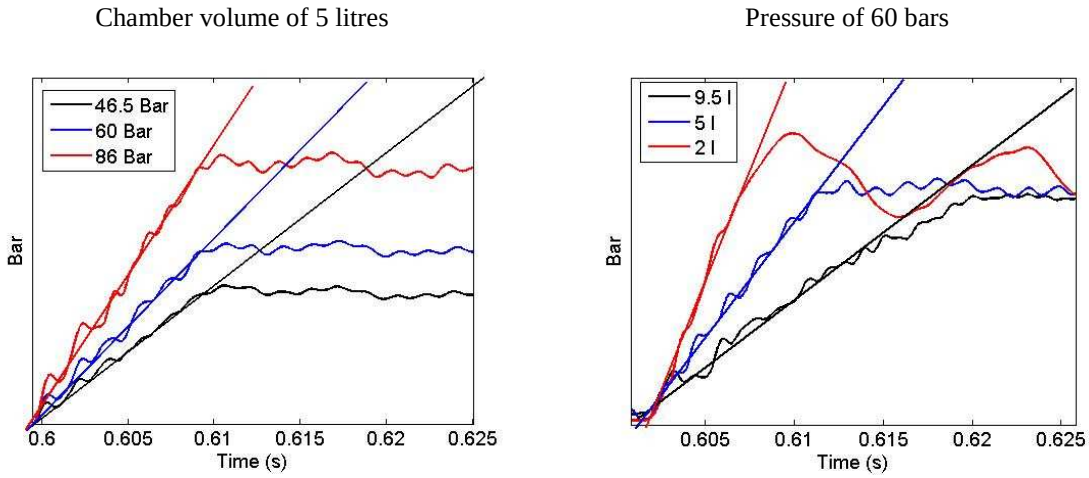

Figure 5: Pressure rise in the generator on the sensor $P_{Chamber\text{-}Div}$.

Figure 6 summarizes the pressure rise measured (i) for a fixed chamber volume of 2 litres, the pressure varying from 46.5 bars to 135 bars, (ii) for a fixed pressure of 60 bars, the chamber volume varying from 2 to 9.5 litres. The gradient pressure in the chamber follows a linear law with the pressure in the tank P_t, with excellent runs repeatability. This linear dependency can be derived from the internal energy of the gas in the chamber, assuming an ideal gas law and an adiabatic expansion in the tank [9]. The gradient pressure versus the chamber volume approximately follows a $1/V$ law. The experiment does not accurately fit this law according to the ideal gas law, because the generator does not exactly work under isotherm conditions. Thus, it seems more reliable to control the pressure gradient, in order to obtain a prescribed value, varying the chamber volume rather than the pressure in the tank.

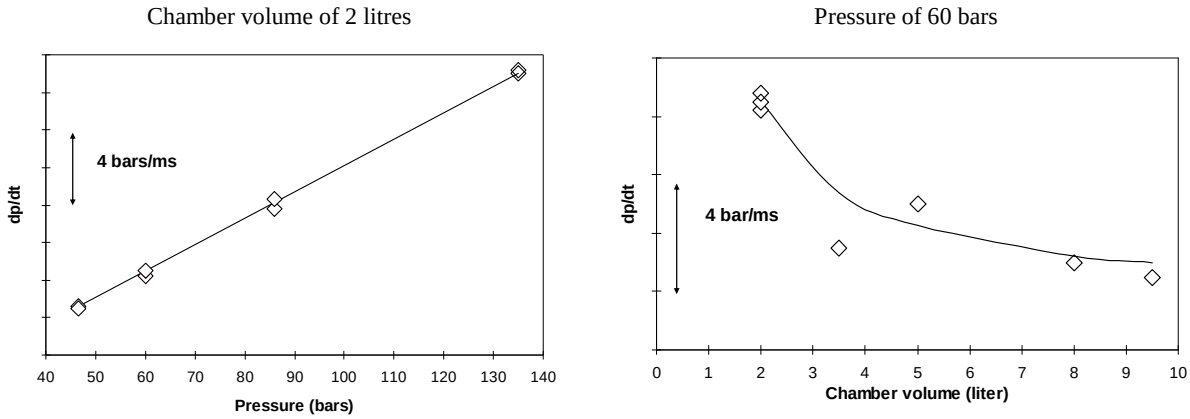

Figure 6: Pressure rise in the generator, $P_{Chamber\text{-}Div}$. ◊ : experiment.

The radiated blast wave is measured on an arc by microphones located from 10 to 70 degrees from the ground and a distance of 4.2 meters (C8 to C2), at the top (L1) and the bottom (L2) of the cylindrical tank and close to the nozzle exit (L3) (see details in figure 10). Figure 7 presents the pressure measured on C2 and C8 microphones for several pressure conditions. The first peak in the signal, an overpressure followed by a depression, corresponds to the incident blast-wave pressure. The second one, on C8, is the reflected field from the ground, this sensor being close to the ground. At the pressure of 46.5 bars, the blast wave magnitude is increased compared to the 25 bars conditions.

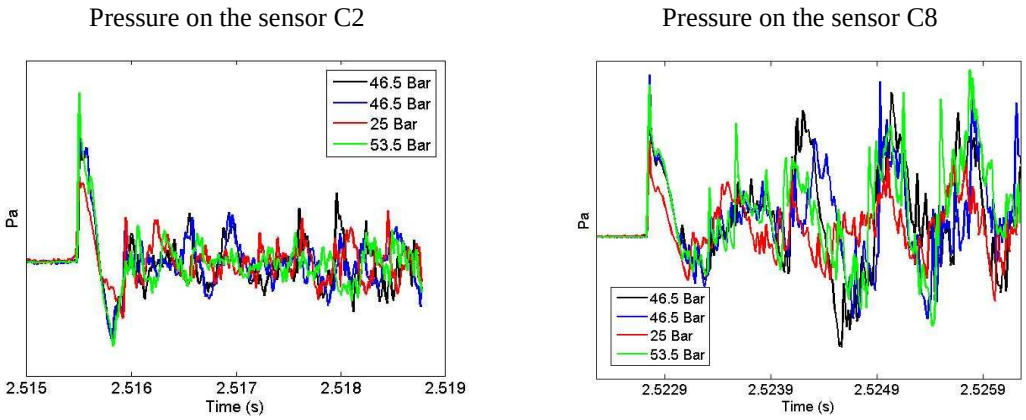

Figure 7: Radiated blast-wave.

Hot gas configuration

First results with the hot gas configuration point out a strong unexpected over pressure on the rise time, measured in the chamber, as illustrated by the black line in figure 8. Such a phenomenon is due to an incomplete combustion of the mixture. This peak is reduced when increasing the pressure and the volume of the chamber due to a more significant combustion; nevertheless several successive adjustments have been performed to overcome this problem. First, an appropriate air and methane injection in the tank has been realized to obtain homogeneous mixture, including the air filling by the top of the tank with a very high mass flow and the filling of the methane by the bottom (air is heavier than methane). The filling of the tank has to be done within few minutes before the ignition to avoid gas stratification. The delay between the ignition of the spark plug in the sphere and the striker order should be typically of few hundred milliseconds to make sure of a complete combustion. A greater delay between these two events may produce a free rupture of the diaphragm, loosing the control of the exact prescribed pressure and of the time sequence. Finally, after each run, immediately, a significant air mass flow (~0.6 kg/s) is blown through the generator – which has no more diaphragm – during 90 seconds, in order to remove the non-negligible condensation and to cool the body of the generator, allowing new tests in a short delay. The red line in figure 8 shows the pressure rise measured by the $P_{Chamber\text{-}Exit}$ sensor, showing the extinction of the peak and small oscillations staying below 10% of the pressure, following the above procedure.

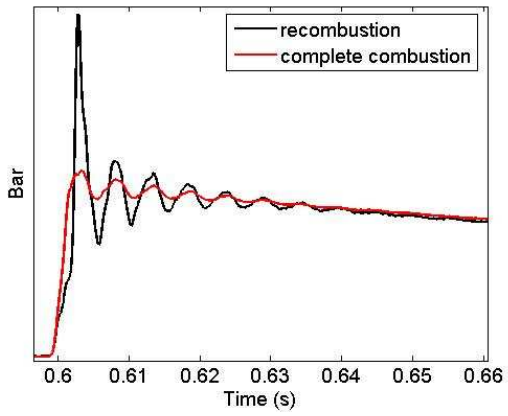

Figure 8: Pressure rise on $P_{Chamber\text{-}exit}$.

Figure 9 details the rise pressure for given volume chamber and tank pressure where, as in Fig. 6, the same concluding remarks can be learned. At constant chamber volume, the pressure rise is nearly linear with the pressure and, at constant pressure; the pressure rise roughly follows a *1/V* law.

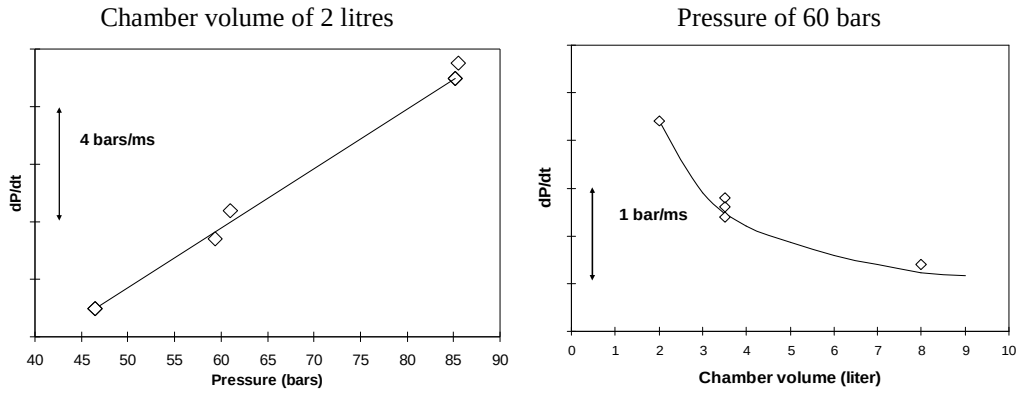

Figure 9: Pressure rise in the generator, $P_{Chamber-Div}$.◊: experiment.

3. Generator in presence of a trench

3.1 Metrology

Figure 3b shows the generator with the trench set up in the Martel facility. A steel plate is located at the level of the trench extension to simulate the ground. Three unsteady pressure sensors are located in the trench (K1, K2, K3) to analyse the blast-wave propagation. 20 microphones are also set up to measure the pressure histories (see Fig. 10):

- an arc of 4 microphones at 4.20 m radius provides the directivity pattern of the DOP (C2, C4, C6 and C8),
- an arc of 3 microphones centred on the nozzle exit at 1,02 m radius provides the directivity pattern of the IOP (C10, C12 and C14),
- 10 microphones around the cylindrical tank measure the pressure close to the generator structure, representative of the loads on the fairing (L1a to L1d, L2a to L2c, L3a to L3d),
- 3 microphones above the trench characterize the propagation from the trench exhaust to the generator (L4 to L6).

Such arrays of sensors ensure an accurate description of the overpressure waves and are also of interest for a detailed comparison between experiment and computation [10].

The metrology outside the trench consists in ¼-in. condenser microphones coupled with a 200 kHz/channel acquisition device, able to store data during some seconds. To allow a nearly real time analysis on the whole sensors, specific routines have been developed. The first step is to synchronize the signals with respect to the peak generated by the diaphragm rupture, being the first and easy event to detect on the L3a signal. The temporal signals are filtered with a low-pass filter at 5 kHz. Due to the large number of sensors, integrated variables are also processed to quickly summarize and validate the results of each run. The maximum and minimum as well as the rms values of the IOP and DOP are stored, providing the directivity pattern of the blast-wave.

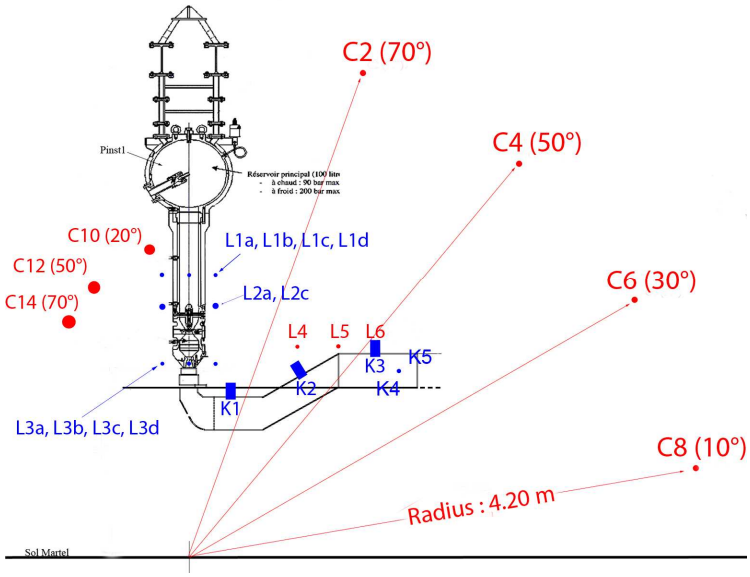

Figure 10: Diagram of the blast generator including the trench and the microphones location

3.2 Blast wave generator in presence of the trench

The blast wave- measured on L1a and C2 microphones is plotted in Fig. 11 for several runs, with the same conditions of pressure and volume chamber. The first peak in the signal represents the IOP and the second one the DOP, at times 0.603 and 0.61 s on L1a, and at times 0.608 and 0.612 s on C2, respectively. The arrival times of these two components are in agreement with the time paths from the nozzle exit and from the duct exit, assuming a practically constant sound celerity. All the runs are performed without recombustion in the chamber following the appropriate procedure to fill the tank, so that a very good repeatability is obtained in view of the complex geometry, a mandatory capability to assess reduction systems. The standard deviation relative to the averaged value is about 10 % for the IOP and 20% for the DOP.

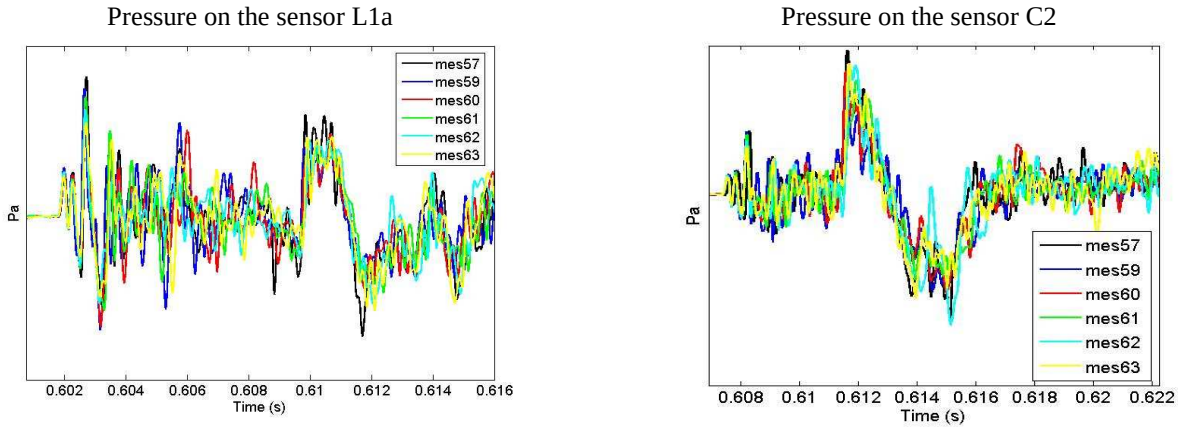

Figure 11: Blast-wave for hot gas in presence of the trench, V = 3.5 l, P = 60 bars.

Comparison between cold and hot gas configurations

Figure 12 compares the cold and the hot overpressure for the same pressure P of 60 bars, in the trench, on K3. The hot gas configuration generates a more intense blast wave, with a ratio of about 2. This is in agreement with the ratio of the internal energy $PV/(\gamma-1)$ of each configuration, where γ represents the specific heat ratio. For the cold gas configuration γ = 1.4, and for the hot gas, the characteristic of the air methane-mixture, determined from the initial conditions (richness of the mixture, initial pressure of 8,5 bars) assuming an isochoric combustion, gives $\gamma \approx 1.2$, so that the ratio of the internal energies for hot and cold gas is 2.

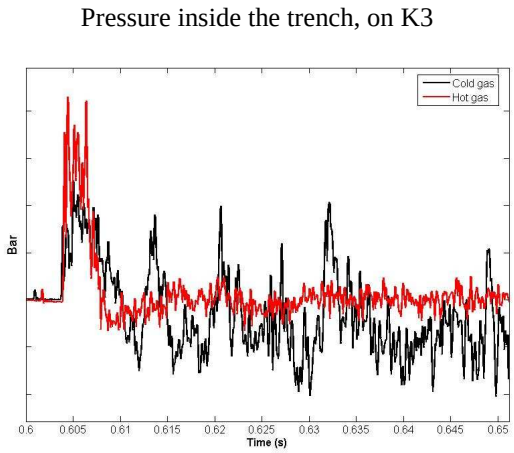

Figure 12: Blast wave in presence of the trench. Comparison between cold and hot gas.

4. Conclusion

The Martel facility funded by CNES and operating since 1996 was first dedicated to research activities on hot supersonic jets. A large amount of test campaigns have been carried out on noise radiated by free jet, impinging supersonic jet and water injection in presence of a trench. The development of a blast wave generator working at cold gas and hot gas based on methane-air combustion constitutes a new system generator in Martel facility. The acceptance of this device shows that the performances of the generator are in agreement with the expected capabilities. The pressure rise in the chamber can be efficiently adjusted thanks to a variable chamber. In presence of the trench, the system exhibits the expected IOP and DOP. An excellent repeatability of this complex blast wave phenomenon is achieved, especially for the hot gas configuration, thanks to an appropriate mixture of the air-methane in the spherical chamber and a well-defined chronology of the two gas injection in the sphere. The blast wave generator is a low cost-in-use and operational device where many parameters can be easily modified, enabling a large number of tests for research activities. First reduction systems including chicanes, deflectors and obstacles have been realized, resulting in a moderate attenuation of the DOP. On the other hand, under study reduction systems based on water injection and spray in the duct are very encouraging, so that future studies will focus on the optimisation of these devices.

Acknowledgements

This work was co-funded by CNES, ASTRIUM and ONERA in the framework of the R&T CNES Program. The authors would like to thank P. Hervat from Onera and D. Desbordes from LCD for their contribution to the technical development of the generator, and its adjustments during the acceptance. Let us thank Ch. Auclercq and J. Lebeau, the technical staff from the MARTEL facility, for their fruitful works during the preparation and the campaigns.

References

[1] Gély D., G. Elias, C. Bresson, H. Foulon, and S. Radulovic. 2000. Reduction of supersonic jet noise:Application to the Ariane 5 launch vehicle, In: *6th AIAA/CEAS Aeracoustics Conference*, 12-14 June, Lahaina, USA.

[2] Colombier, R; and M. Pollet. 1991. Solid rocket motor ignition overpressure prediction, AIAA-1991-2437, *27th Joint propulsion Conference*, 26-28 June, Sacramento, CA, USA.

[3] Ikawa, H., F., and P.Laspesa. 1985. Ignition/duct Overpressure Induced by Space Shuttle Solid Rocket motor Ignition. *J. Spacecraft*, 22: 481-488.

[4] Brenner, P, and M. Pollet. 2005. Highly unsteady flows about bodies in relative motion. In: *Colloque AAAF: Aérodynamique instastionnaire*, Toulouse, France.

[5] Tsustumi, S., R. Takaki, E. Shima, K. Fujii, and M. Arita. 2008. Generation and propagation of pressure waves from H-IIA launch vehicle at lift-off. In: *46th AIAA Aerospace Sciences Meeting and Exhibit*, 7-10 January, Reno, Nevada, USA.

[6] Varnier, J, P. Prévot, G. Dunet, M. Barat, and B. Mazin. 2006. Blast wave and afterburning at ignition of rocket engines. In: *13th International Congress on Sound and Vibration*, ICSV13, 2-6 July, Vienna, Austria.

[7] Troyes, J., F. Vuillot, J. Varnier, and P. Malbéqui. 2009. Numerical simulations of rocket solid motor engine ignition and duct overpressure waves at reduced scale. In: *45th AIAA/ASME/SAE/ASEE Joint Propulsion Confererence and Exhibit*, Denvers, USA.

[8] Troyes, J.,V Vuillot, and J.-B. Dargaud. 2010, Numerical simulations of model solid rocket motor ignition overpressure waves. Part II Vertical firing with flame duct. In: *17th International Congress on Sound & vibrations*, ICSV17, 18-22 July, Cairo, Egypt.

[9] M. Pollet. 2009. Programme recherche et technologie lanceurs, Pole AEID, Onde De Souffle au décollage. Etat du banc Martel : analyse de la campagne de mise au point C1 – Gaz froids – Gaz chauds, EADS-Astrium, RT-NT-411-0902-EADS-01.

[10] Jouy, B., J. Troyes, J.-B. Dargaud, and F.Vuillot. 2011. Numerical simulation of the overpressure at Martel facility: combustion and wave generation. In: *4th European Conference for Aerospace Sciences*, EUCASS, 4-8 July, Saint-Petersburg, Russia.